The 5th Student Conference on Research and Development –SCOReD 2007
11-12 December 2007, Malaysia

Sliding Mode Control with Linear Quadratic Hyperplane Design: An application to an Active Magnetic Bearing System

A. R. Husain, *Student Member, IEEE*, M. N. Ahmad and A. H. Mohd. Yatim, *Senior Member, IEEE*

***Abstract*-- This paper deals with modeling and control of a nonlinear horizontal active magnetic bearing (AMB) system via current control scheme. The gyroscopic effect and mass imbalance inherited in the system are proportional to the rotor speed in which these nonlinearities cause high system instability as the rotational speed increases. In order to synthesize a robust controller that can stabilize the system under a wide range of rotational speed, the dynamic AMB model is transformed into a deterministic model to form a class of uncertain system. Then, based on Sliding Mode Control (SMC) theory and Lyapunov method, a new robust controller that stabilizes the system is proposed wherein the Linear Quadratic Regulator (LQR) is used to design the sliding surface. Under this control, the reaching condition is guaranteed and the closed loop system is stable. The performance of the controller applied to the AMB model is demonstrated through simulation works under various rotational speeds and system conditions.**

***Index Terms*—Active Magnetic Bearing (AMB), Sliding Mode Control, deterministic form.**

I. Introduction

SLIDING Mode Control (SMC) has received great attention in recent years because of its robustness against uncertainties that present in system [1], [2] and [3]. SMC is a nonlinear control technique that is applicable to linear, nonlinear, multi-input/multi-output, discrete-time and large scale systems. There are many approaches which have been considered in the design process of the sliding-mode control law, such that the system is robust or even insensitive to parametric uncertainties and disturbance.

In the practical application of SMC, the controller has been successfully adapted in many forms and applied in numerous real-world applications such as DC-motor control [4], robot manipulator [5], active suspension system [6], magnetic suspension system and magnetic bearings [7][8].

Prior designing the SMC control law, a representation of the dynamic system in a class of model structure is a prerequisite for development of the control algorithm. Once the model is available, the design of SMC controller involves two crucial steps which are commonly referred to as the reaching phase and the sliding phase [2][9]. In this paper, the design of both the sliding surface and control law based on SMC theory and its application to a four-degree-of-freedom (DOF) AMB system are considered. The AMB system contains the gyroscopic effect and imbalance in which this nonlinearities cause the system to be unstable and the magnitude is proportional to the rotating speed of the rotor. The designed controller is proven to be able to stabilize the AMB system for a given range of rotational speed, which is a main advantage compared to the method reported in [8]. In addition, instead of using the standard pole placement method to parameterize the sliding surface, an optimal quadratic method in which the linear quadratic performance index is minimized. The hyperplane design problem as shown in [10] is finally reduced to be a standard Linear Quadratic Regulator (LQR) problem in which the design procedure is quite established. The stability of the closed-loop system is guaranteed and the whirling orbit of the rotor due to the nonlinearities is reduced significantly.

The outline of this paper is as follows: In Section II, the model of the AMB system based on [8] is illustrated and represented in its deterministic form which serves as a tool for the controller design. Section III covers the detail design of SMC control algorithm wherein both the parameterization of sliding surface based on LQR method and the development of nonlinear control law are shown. The stability of the system under the designed controller is also proven mathematically. Then, in Section IV, the performances on the AMB system under the controller are illustrated through simulation works under various system conditions. Finally, the conclusion in Section V summarizes the contribution of the work.

II. Modeling of An Active Magnetic Bearing System

In order to synthesize the proposed sliding surface with the controller, a vertical shaft AMB system model for the application of turbo molecular pump system is re-derived based on the work done in [8].

This work was supported in part by the Ministry of Science, Technology and Innovation (MOSTI) Malaysia under grant ScienceFund No.79014.

A. R. Husain is with the Mechatronic and Robotic Dept., Faculty. of Elec. Eng. UTM, Skudai, Johore, Malaysia (e-mail: rashid@fke.utm.my).

M. N. Ahmad is the Head of Mechatronic and Robotic Dept., Faculty. of Elec. Eng. UTM, Skudai, Johore, Malaysia (e-mail: noh@fke.utm.my).

A. H. Mohd. Yatim is the Deputy Dean (Academic) at Faculty of Elec. Eng. UTM, Skudai, Johore, Malaysia (e-mail: halim@ieee.org).

1-4244-1470-9/07/$25.00 ©2007 IEEE.

A. Mathematical Model

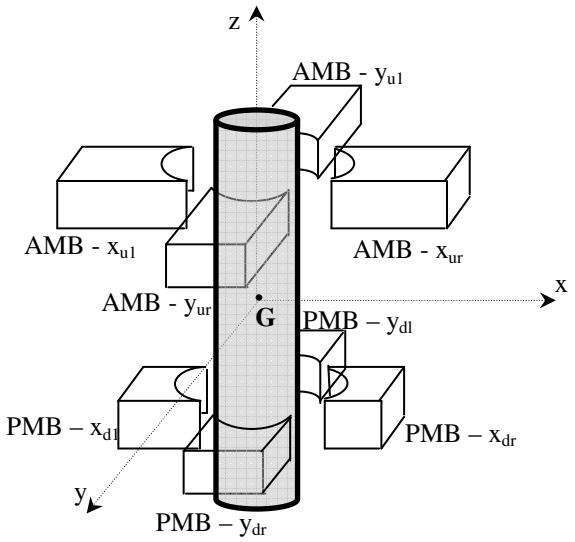

Fig. 1. Vertical Active Magnetic Bearing System

The gyroscopic effect that causes the coupling between two axes of motions (pitch and yaw) is also considered. Fig. 1 illustrates the five degree-of-freedom (DOF) vertical magnetic bearing in which the vertical axis (z-axis) is assumed to be decoupled from the system and hence controlled separately.

The top part of the rotor of the system in Fig. 1 is controlled actively by the magnetic bearing, labeled as AMB, in which the coil currents are the inputs. The bottom part of the rotor however is levitated to the center of the system by using two sets of permanent magnets labeled as PMB. The rotation of rotor around the z-axis is supplied by external driving mechanism and considered a time-varying parameter. Fig. 2 illustrates the free-body diagram of the rotor which shows the total forces produced by the AMB and PMB of the system. Based on the principle of flight dynamics [11], the equations of motion of the rotor-magnetic bearing system is as follows:

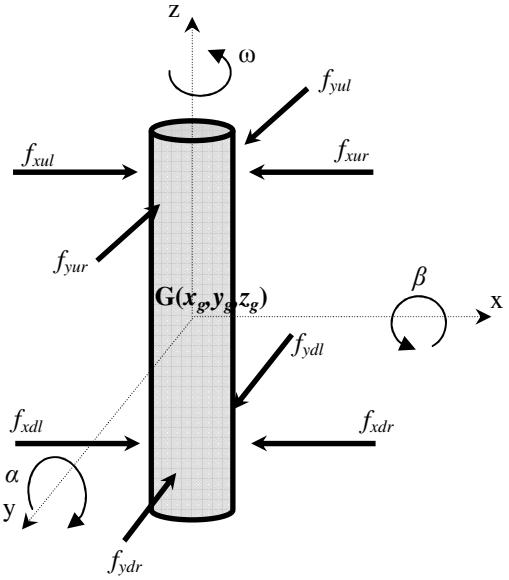

Fig. 2. The total forces acting on the AMB rotor.

$$\begin{aligned} m\ddot{x}_g &= f_{x_u} + f_{x_b} + m_{un} l\omega^2 \cos(\omega t) \\ J_r\ddot{\beta} &= -J_a\omega_z\dot{\alpha} + L_u f_{x_u} - L_b f_{x_b} \\ m\ddot{y}_g &= f_{y_u} + f_{y_b} + m_{un} l\omega^2 \sin(\omega t) \\ J_r\ddot{\alpha} &= J_a\omega_z\dot{\beta} - L_u f_{y_u} + L_b f_{y_b} \end{aligned} \tag{1}$$

The terms $m_{un} l\omega^2 \cos(\omega t)$ and $m_{un} l\omega^2 \sin(\omega t)$ are the imbalances due the difference between rotor geometric center and mass center. These imbalances cause the whirling motion and the magnitude is proportional to the rotor rotational speed, ω. The gyroscopic effect is represented by the term $-J_a\omega_z\dot{\alpha}$ and $J_a\omega_z\dot{\beta}$, where it can be noticed that this will cause the coupling between the axes of motions proportional to the speed. The control forces produced by the AMB are given by the following equations:

$$\begin{aligned} f_{xu} &= 2K_{du}x_g + 2L_u K_{du}\beta + 2K_{iu}i_{xu} \\ f_{yu} &= 2K_{du}y_g - 2L_u K_{du}\alpha + 2K_{iu}i_{yu} \end{aligned} \tag{2}$$

where $f_{xu} = f_{xur} - f_{xul}$ and $f_{yu} = f_{yur} - f_{yul}$ are the net forces produced by the AMB on each *x*- and *y*-axis respectively (the same net force for bottom PMB as well). This is possible by having the AMB coil wound to produce differential current mode. For the PMB, the net forces produced are given by the following equations:

$$\begin{aligned} f_{xb} &= -2C_b\dot{x}_g + 2C_b L_b\dot{\beta} - 2K_b x_g + 2K_b L_b\beta \\ f_{yb} &= -2C_b\dot{y}_g - 2C_b L_b\dot{\alpha} - 2K_b y_g - 2K_b L_b\alpha \end{aligned} \tag{3}$$

Equations (1), (2) and (3) can be integrated to produce the AMB model in the following form:

$$\dot{X}(t) = A(\omega)X(t) + BU(t) + F(\omega,t) \tag{4}$$

where $X = [x_g, \beta, y_g, \alpha, \dot{x}_g, \dot{\beta}, \dot{y}_g, \dot{\alpha}]^T$ are the states of the system, $A(\omega) \in \Re^{8x8}$ is the system matrix, $B \in \Re^{8x2}$ is the input matrix, $U(t) = [i_{xu}\ i_{yu}]^T$ the input currents and $F(\omega,t)$ is the disturbance vector due to the imbalances. The nonzero elements of the matrices are shown in the appendix.

B. AMB model in deterministic form

In order to synthesize the controller, the AMB model is treated as an uncertain system in which deterministic approach to classify the system is used based on [12]. By using this approach, the AMB model can be decomposed into its nominal and uncertain part as shown below

$$\dot{X}(t) = (A + \Delta A(\omega,t))X(t) + BU(t) + F(\omega,t) \tag{5}$$

where $\Delta A(\omega,t)$ represents the uncertainty of the system matrix and $F(\omega,t)$ is the disturbance matrix associated with speed dependent of imbalance. A and B are the nominal constant matrices of the system. The decomposition into this deterministic form is possible due to the fact that the maximum and minimum values of the rotational rotor speed are known. The elements of the $\Delta A(\omega,t)$ and $F(\omega,t)$ can be calculated

based on these available bounds. The rotational speed is given as follows:

$$0 \ rad/\sec \le \omega \le 3142 \ rad/\sec . \quad (6)$$

Then, by using these bounds and the other system parameter values as shown in Table I, each element of the system and disturbance matrices can be calculated and specified in the following form:

$$\underline{a}_{ij} \le a_{ij}(\omega,t) \le \overline{a}_{ij} \quad (7a)$$

$$\underline{d}_j \le d_j(\omega,t) \le \overline{d}_j \quad (7b)$$

for i = 1, …, 8, and j = 1, …, 8, where $a_{ij}(\omega,t)$ and $d_j(\omega,t)$ are the element of $\Delta A(\omega,t)$ and $F(\omega,t)$ matrices respectively. The upper and lower bars indicate the maximum and minimum values of the elements. The element of matrix A and $\Delta A(\omega,t)$ can be calculated based on these bounds by using the following procedure:

$$a_A(i,j) = \frac{\overline{a}_{ij} + \underline{a}_{ij}}{2}, \ a_{\Delta A}(i,j) = \overline{a}_{ij} - a_A(i,j) \quad (8)$$

for i-th row,j-th column elements of A and $\Delta A(\omega,t)$.

For the disturbance matrix, $F(\omega,t)$, only the maximum values of the elements are needed since these values represent the highest disturbance values caused by the imbalance which should be eliminated from the system.

TABLE I
PARAMETER FOR VERTICAL AMB SYSTEM [8]

Symbol	Parameter	Value	Unit
m	Mass of Rotor	1.595	kg
J_a	Moment of Inertia about rotational axis	1.61×10^{-3}	kg.m^2
J_r	Moment of Inertia about radial axis	3.83×10^{-3}	kg.m^2
L_u	Distance of upper AMB to G	0.0128	m
L_b	Distance of lower PMB to G	0.0843	m
K_{iu}	Linearized force/current factor	200	N/A
K_{du}	Linearized force/displ. factor	2.8×10^5	N/m
K_b	Stiffness coefficient of PMB	1.0×10^5	N/m
C_b	Damping coefficient of PMB	48	kg/s
m_{un}	Static imbalance	0.6×10^{-3}	m
l	Distance of unbalance mass from G	0.02	m
ω	Rotor rotational speed	0 – 1047 (0 – 10000)	rad/sec (rpm)

III. SLIDING MODE CONTROLLER DESIGN

Consider a dynamical system modeled by the following differential equation

$$\dot{x}(t) = (A + \Delta A(\omega,t))x(t) + Bu(t) + F(\omega,t) \quad (9)$$

where $x(t) \in \Re^n$ is the system states, $u(t) \in \Re^m$ is the control input, $F(\omega,t)$ is the nonlinear disturbance that presents in the system and matrix B is of full rank. $\Delta A(\omega,t)$ is the uncertainty in the system matrix. To complete the description of the uncertain dynamical system, the following assumptions are introduced and assumed to be valid.

A1) For existence purposes, $\Delta A(\cdot,\cdot)$ and $F(\cdot,\cdot)$ are continuous on their arguments.

A2) Matching condition is met and there exist functions $H(p,t): \Re \times \Re^n \to \Re^{m \times n}$ and $E(p,t): \Re \times \Re^n \to \Re^m$ such that

$$\Delta A(\omega,t) = BH(\omega,t)$$
$$F(\omega,t) = BE(\omega,t)$$

A3) The pair (A,B) is completely controllable.

From the structural assumptions, the uncertainties can be lumped and the dynamical system can be represented in the following form:

$$\dot{x}(t) = Ax(t) + B[u(t) + g(\omega,t)] \quad (10)$$

where $g(\omega,t)$ is the lumped uncertainties. Notice that the system varies with the time-varying parameter, ω, and if the bound is known, the following assumption can be introduced.

A4) There exists a positive scalar valued function $\rho(\omega,t): \Re \times \Re \to \Re_+$ such that $\|g(\omega,t)\| \le \rho(\omega,t)$.

A. Sliding surface design

In SMC design, the first step is to parameterize the sliding surface such that the system constrained to the sliding surface exhibits desired system behavior. As covered in [2],[9] and [10], under the SMC, once the system slides on the designed surface, the order of the system is reduced. This can be demonstrated by treating $g(\omega,t) = 0$ in (10) and the nominal system now can be partitioned and represented as follows:

$$\begin{bmatrix} \dot{x}_1 \\ \dot{x}_2 \end{bmatrix} = \begin{bmatrix} A_{11} & A_{12} \\ A_{21} & A_{22} \end{bmatrix} \begin{bmatrix} x_1 \\ x_2 \end{bmatrix} + \begin{bmatrix} 0 \\ B_1 \end{bmatrix} u(t) \quad (11)$$

where $x_1 \in \Re^{(n-m)}$ and $x_2 \in \Re^m$. Let the sliding surface is defined to be as follows:

$$\sigma(t) = \{ x \in \Re^n : Sx(t) = 0 \} \quad (12)$$

where $S \in \Re^{m \times n}$ is full rank matrix, $S = [S_1 \ S_2]$ and $S_2 \in \Re^{m \times m}$ is nonsingular. Thus, during the ideal sliding, the motion can be represented as

$$S_1 x_1 + S_2 x_2 = 0$$

$$x_2 = -\frac{S_1}{S_2} x_1 = -Mx_1 . \quad (13)$$

Based on (11), the closed loop system on the sliding surface is given by

$$\dot{x}_1 = A_{11}x_1 - A_{12}x_2 . \quad (14)$$

Substituting (13) into (14), the closed-loop system is represented as follows:

$$\dot{x}_1 = (A_{11} - A_{12}M)x_1 \quad (15)$$

It is clear the closed-loop system will be stable as long as the eigenvalues of (A_{11}-$A_{12}M$) are stable, i.e. the eigenvalues are on the left-hand side of the s-plane. This can be achieved by choosing the design matrix M through various linear state feedback control laws including pole placement method, quadratic minimization and direct eigenstructure assignment [10]. In this work, the design of the sliding surface subjected to minimization of the following quadratic performance index is considered [10]:

$$J = \frac{1}{2}\int_{t_s}^{\infty} x(t)^T Qx(t)dt \quad (16)$$

where Q is symmetric positive definite, and t_s is the time when the sliding motion starts. To continue with the design, matrix Q is partitioned such that it is compatible with the reduced order system (11) and given as follows:

$$Q = \begin{bmatrix} Q_{11} & Q_{12} \\ Q_{21} & Q_{22} \end{bmatrix} \quad (17)$$

where $Q_{12} = Q_{21}$. Equation (16) can now be transformed to match the structure of the system (11) and can be expressed as

$$\begin{aligned} J &= \frac{1}{2}\int_{t_s}^{\infty} (x_1{}^T Q_{11}x_1 + x_1{}^T Q_{12}x_2 + x_2{}^T Q_{21}x_1 + x_2{}^T Q_{22}x_2)\,dt \\ &= \frac{1}{2}\int_{t_s}^{\infty} (x_1{}^T Q_{11}x_1 + 2x_1{}^T Q_{12}x_2 + x_2{}^T Q_{22}x_2)\,dt \end{aligned} \quad (18)$$

Equation (18) can be treated as a standard LQR problem when the last two terms of (18) are factored out as follows:

$$\begin{aligned} 2x_1{}^T Q_{12}x_2 + x_2{}^T Q_{22}x_2 = (x_2 + Q_{22}^{-1}Q_{21}x_1)^T Q_{22}(x_2 + Q_{22}^{-1}Q_{21}x_1) \\ - x_1^T Q_{21}^T Q_{22}^{-1} Q_{21}x_1 \end{aligned} \quad (19)$$

Substituting (19) into (18) yields

$$\begin{aligned} J &= \frac{1}{2}\int_{t_s}^{\infty} x_1{}^T (Q_{11} - Q_{12}Q_{22}^{-1}Q_{21})x_1 \\ &\quad + (x_2 + Q_{22}^{-1}Q_{21}x_1)^T Q_{22}(x_2 + Q_{22}^{-1}Q_{21}x_1)dt \\ &= \frac{1}{2}\int_{t_s}^{\infty} (x_1{}^T \overline{Q}x_1 + z^T Q_{22}z)dt \end{aligned} \quad (20)$$

where

$$\overline{Q} = Q_{11} - Q_{12}Q_{22}^{-1}Q_{21} \quad (21)$$

$$z = x_2 + Q_{22}^{-1}Q_{21}x_1 . \quad (22)$$

Recall that the dynamic of the reduced order system during the sliding motion is represented by (14). By using (22), x_2 can be eliminated and the new reduced order system can be shown as follows:

$$\dot{x}_1 = (A_{11} - A_{12}Q_{22}^{-1}Q_{21})x_1 + A_{12}z \quad (23)$$

Notice that with minimization of cost function (20) subject to system (23) is similar to the standard LQR problem in which $Q_{22} > 0$ since Q is selected to be positive definite. This condition guarantees the existence of Q_{22} and $\overline{Q} > 0$. Approaching the design problem in similar line with LQR problem, the optimal z that minimizes (20) is given as follows:

$$z = -Q_{22}^{-1}A_{12}^T Px_1 \quad (24)$$

where P is the unique solution of the algebraic Riccati equation (ARE) given by

$$P(A_{11} - A_{12}Q_{22}^{-1}Q_{21}) + (A_{11} - A_{12}Q_{22}^{-1}Q_{21})^T P - PA_{12}Q_{22}^{-1}A_{12}^T P + \overline{Q} = 0 \quad (25)$$

Substituting (24) into (22) will result

$$\begin{aligned} Q_{22}^{-1}A_{12}^T Px_1 &= -x_2 - Q_{22}^{-1}Q_{21}x_1 \\ x_2 &= -Q_{22}^{-1}(A_{12}^T Px_1 + Q_{21})x_1 \\ &= -Mx_1 \end{aligned} \quad (26)$$

which is equivalent to (13). Thus, finding the solution of (26) leads to the values of the sliding surface parameter, S.

B. Control law design

The next crucial step is to establish a control law such that the reachability condition, $\sigma^T\dot{\sigma} < 0$ is met. When this condition is fulfilled, the system states trajectories are attracted to the designed surface and on the intersection with the surface, the trajectories will remain there for all subsequent time [2][10]. Based on this methodology, the following proposition is stated.

Proposition 3.1. Given a class of uncertain system (10), the reaching condition $\sigma^T\dot{\sigma} < 0$ is satisfied by employing the control law $u(t)$ given below:

$$u(t) = -(SB)^{-1}K\sigma - (SB)^{-1}SAx - \rho(\omega,t)\frac{B^T S^T \sigma}{\left\|B^T S^T \sigma\right\|} \quad (27)$$

where $K \in \Re^{m\times m}$ is a positive design matrix.

Proof: Given the uncertain system (10), the reachability condition evaluates to

$$\begin{aligned} &\sigma^T\dot{\sigma} = \sigma^T S(Ax(t) + B[u(t) + g(\omega,t)]) \\ &= \sigma^T SAx(t) + \sigma^T SB[u(t) + g(\omega,t)] \\ &= \sigma^T SAx(t) + \sigma^T SB[-(SB)^{-1}K\sigma - (SB)^{-1}SAx - \rho(\omega,t)\frac{B^T S^T\sigma}{\left\|B^T S^T\sigma\right\|}] \\ &\quad + \sigma^T SBg(\omega,t) \end{aligned}$$

$$= \sigma^T SAx(t) - \sigma^T SB(SB)^{-1} K\sigma - \sigma^T SB(SB)^{-1} SAx - \rho(\omega,t)\frac{\sigma^T SBB^T S^T \sigma}{\left\|B^T S^T \sigma\right\|}]$$

$$+ \sigma^T SBg(\omega,t)$$

$$< -\sigma^T K\sigma - \rho(\omega,t)\frac{\left\|B^T S^T \sigma\right\|^2}{\left\|B^T S^T \sigma\right\|} + \left\|\sigma^T SB\right\|\rho(\omega,t)$$

$$< -\sigma^T K\sigma$$

Thus, the condition $\sigma^T \dot{\sigma} < 0$ is met as long as the matrix K is chosen to be positive definite. If $K = I$ is selected, then the following is true:

$$\sigma^T \dot{\sigma} < -\sigma^T \sigma < \left\|\sigma^2\right\|$$

This completes the proof. □

Notice that the control law (27) has the constant gain, $\rho(\omega,t)$, obtained from the norm bounded lumped uncertainty. By looking at the dynamical system (9), however, the nonlinearity of disturbance term, $F(\omega,t)$, can be treated as an external disturbance which depends on the time-varying parameter. Applying this idea to the AMB model developed earlier, the time varying parameter is the rotational speed and it varies from zero to 10000rpm. Thus, if the constant gain $\rho(\omega,t)$ is designed such that

$$\rho(\omega,t) = \rho_A(\omega,t) + \omega\,\rho_f(\omega,t) \qquad (28)$$

where $\rho_A(\omega,t)$ is a constant gain that bound the system uncertainty and $\omega\rho_f(\omega,t)$ is a time-varying parameter dependent gain that bound the disturbance effect with ω remains as the time-varying parameter. With this newly defined gain, the previous proposition is restated:

Proposition 3.2. For the uncertain dynamical system of class (10), which is equivalent to system (11), the control law (27) with the controller gain (28) can satisfy the reachability condition $\sigma^T \dot{\sigma} < 0$.

Proof: The proof is omitted since it is in similar line of proof for *Proposition 3.1*. □

The main advantage of having this new control law is the control input can be adapted according to the time-varying parameter in which this will reduce the conservatism of having norm-bounded disturbance that accommodates the maximum disturbance value. However, the trade-off is the new control law needs an on-line update of the time-varying parameter for the gain calculation where it might be unrealistic for certain dynamical system. Looking specifically for the AMB application, however, the time-varying rotational speed is practically available through online measurement and does not impose any constraint in implementation wise.

IV. Simulation Result And Discussion

The simulation work is performed by using MATLAB® and Simulink®. After transforming the AMB model into the deterministic form, the procedure of designing the controller and its application on the system is outlined as follows:

***Step 1*:** Compute the norm for the system matrix uncertainty $\Delta A(\omega,t)$, matrix B and disturbance vector $F(\omega,t)$.

$$\left\|\Delta A\right\| = 220.0614\ ,\ \left\|B\right\| = 1.3601\times10^3, \left\|F(p,t)\right\| = 8.2479$$

Note that for controller (27) with gain (28), the norm of disturbance is not required since the value of $\rho_f(\omega,t)$ can be obtained from the value of the mass imbalance. The norm value is shown here to show the magnitude of the disturbance relative to the gyroscopic effect in the matrix uncertainty.

***Step 2*:** Compute the gain (27) with mass imbalance, $m_{un} = 0.6 \times 10^{-3}$ kg.

$$\rho_A \geq \left\|H(p,t)\right\| = \frac{\left\|\Delta A(p,t)\right\|}{\left\|B\right\|} = \frac{220.0614}{1.3601\times10^3} = 0.162$$

$$\rho_f \geq \frac{\frac{m_{un}}{m} l}{\left\|B\right\|} = \frac{7.524\times10^{-6}}{1.3601\times10^3} = 5.532\times10^{-9}$$

Also notice that although the gain ρ_f is considerably small, the final value of the gain will increase as the speed increases. As highlighted earlier, this gain is zero if no imbalance presents and the total control effort is reduced and mainly contributed by the equivalent control term.

***Step 3*:** Parameterize the sliding surface matrix, S. From (13) the parameter S_2 acts as a scaling parameter and does not give any impact on the stability of the closed-loop system (15). Thus S_2=I is chosen. For matrix S_1, the matrix M is calculated based on (26). From the structure of matrix Q shown by (17) and its positive definiteness, Q is chosen such that of, $Q_{12} = Q_{21} = 0$, Q_{11} = diag{2000,100,100,100} and Q_{22} = diag{10^{-6}, 10^{-6}, 10^{-6}, 10^{-6}}. Notice that $Q_{22} = 0$ can still guarantee the positive definiteness of Q, however, small values of Q_{22} is selected to ensure the existence of (20). With these design values, the value for 'gain' matrix M and the resulted sliding surface parameters are as follows:

$$M = \begin{bmatrix} 0 & 0 & 10^4 & 0 & 0 \\ -1.5103\times10^6 & -3.0056\times10^4 & 0 & 10^4 & -2.4448\times10^3 \\ & & & & 0 \\ & & & & -48.621 \end{bmatrix}$$

$$S_1 = M$$

since $S_2 = I$.

In order to view the performance of the controller, the system is run at three different rotating speed and the resonant frequency (critical speed) at ω = 6000rpm as stated in [8] where the system produces the most chaotic whirling motion and the largest whirling rotor orbit. In Fig. 4, the largest diameter of the whirling rotor orbit is about 7μm, achieving a about 90% reduction of rotor orbit compared to the result in [8] shown in Fig. 3. To further compare the performance of the controller, the diameter of the rotor orbit at speed ω = 8000rpm and ω =10000rpm are also shown in Fig. 5 and Fig. 6 respectively wherein the decrease of the diameters of the rotor orbit are significantly achieved.

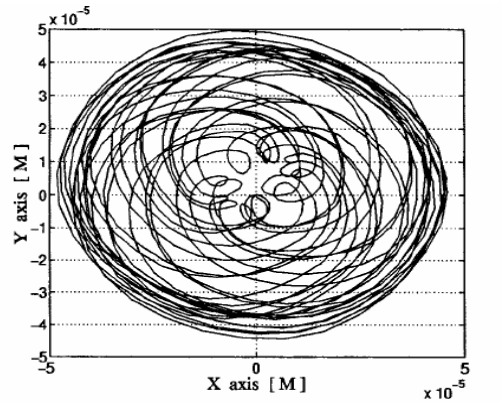

Fig. 3. X-Y displacement of rotor at speed, ω=6000rpm from [8].

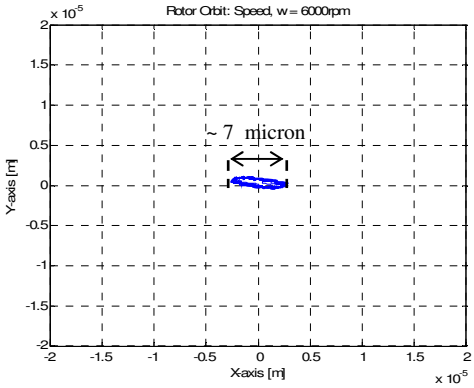

Fig. 4. X-Y displacement of rotor at speed, ω=6000rpm.

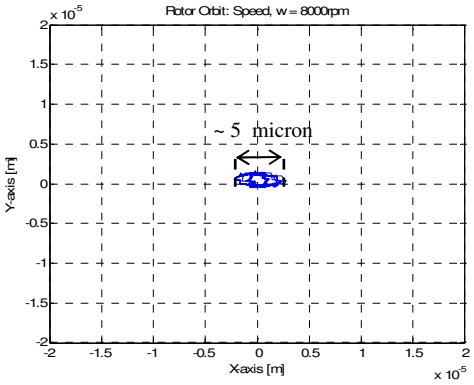

Fig. 5. X-Y displacement of rotor at speed, ω =8000rpm.

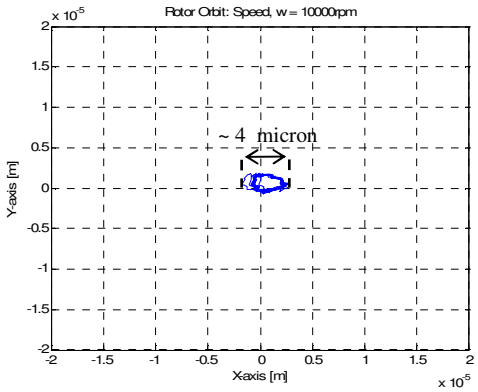

Fig. 6. X-Y displacement of rotor at speed, ω =10000rpm.

V. Conclusion

In this work, a new SMC controller is proposed for stabilization of a four-DOF AMB system in which sliding surface is designed based on LQR method. The proposed controller is proven to be more superior in term of eliminating the whirling motion of the rotor at wide range of rotational speed as compared to method in [8] and this is demonstrated through various simulation results.

VI. Appendix

The nonzero elements of matrix $A(\omega,t)$, B and $F(\omega,t)$ where i and j indicate the i-th and j-th entry of each element.

$$a_{51}=\frac{2(K_{du}-K_b)}{m}, a_{52}=\frac{2(L_uK_{du}-L_bK_b)}{m}, a_{55}=\frac{2C_b}{m}, a_{56}=\frac{2C_bL_b}{m},$$

$$a_{61}=\frac{2(L_uK_{du}-L_bK_b)}{J_r}, a_{62}=\frac{2(L_u^2K_{du}-L_b^2K_b)}{J_r}, a_{65}=\frac{2L_bC_b}{J_r},$$

$$a_{66}=\frac{2L_b^2C_b}{J_r}, a_{68}=\frac{J_a}{J_r}p, a_{73}=\frac{2(K_{du}-K_b)}{m}, a_{74}=\frac{2(L_uK_{du}+L_bK_b)}{m},$$

$$a_{77}=\frac{2C_b}{m}, a_{78}=\frac{2C_bL_b}{m}, a_{83}=\frac{2(L_uK_{du}+L_bK_b)}{J_r}, a_{84}=\frac{2(L_u^2K_{du}-L_b^2K_b)}{J_r},$$

$$a_{86}=\frac{J_a}{J_r}p,\ a_{87}=\frac{2L_bC_b}{J_r}, a_{68}=\frac{2L_b^2C_b}{J_r}, b_{51}=b_{72}=\frac{2K_{iu}}{m}, b_{61}=-b_{82}=\frac{2L_uK_{iu}}{J_r},$$

$$f_5=\frac{m_{un}}{m}l\omega^2\cos(\omega t), f_7=\frac{m_{un}}{m}l\omega^2\sin(\omega t)\cdot$$

VII. References

[1] G. Wheeler, C. Y. Su and Y. Stepanenko, "A Sliding Mode Controller with Improved Adaptation Laws for the Upper Bounds on the Norm of Uncertainties," *Automatica*, Vol 34. No. 12, 1998, pp. 1657-1661.

[2] R.A. DeCarlo, S.H. Zak and G.P. Matthews, "Variable Structure Control of Nonlinear Multivariable System: A Tutorial", Proc. *IEEE,* vol 48, , Mar. 1988, pp. 212-232.

[3] X. Li and R.A DeCarlo, "Robust Sliding Mode Control of Uncertain Time Delay Systems", *Int. J. Control*, vol. 76(13), 2003, pp. 1296-1305.

[4] H.-S. Choi, Y. –H. Park, Y. Cho and M. Lee, "Global Sliding Mode Control: Improved Design for a Brushless DC Motor, " *IEEE Contr. Sys. Mag*., June 2001, pp. 27-35.

[5] M. N. Ahmad, J. H. S. Osman and M. R. A. Ghani, "Proportional-Integral Sliding Mode Tracking Controller with Application to a Robot Manipulator," *7th Int. Conf., ICARCV* 2002, pp. 863-868.

[6] Y. M. Sam and J.H.S. Osman, "Modeling and Control of Active Suspension System Using Proportional Integral Sliding Mode Approach, " *Asian Jour. Contr*., vol. 7(2), June 2005, pp. 91-98.

[7] J. H. Lee, P. E. Allaire, G. Tao, J. A. Decker and X. Zhang, "Experimental Study of Sliding Mode Control for a Benchmark Magnetic Bearing System and Artificial Heart Pump Suspension," *IEEE Trans. on Contr. Sys. Mag*, vol. 11(1), Jan. 2003, pp.128-138.

[8] S. Sivrioglu and K. Nonami, " Sliding Mode Control With Time-Varying Hyperplane for AMB Systems," *IEEE/ASME Trans. on Mechatronics*, vol. 3(1), Mar. 1998, pp. 51-59.

[9] J. Y. Hung, W. B. Gao and J. C. Hung, "Variable Structure control: A Survey," *IEEE Trans. Ind. Electron.* Vol. 40(1), Feb 1993, pp. 2-22.

[10] S. Spurgeon and. C. Edwards, Sliding Mode Control: Theory and Applications., *Taylor and Francis*, London, 1998.

[11] F. Matsumura, and T. Yoshimoto,"System modeling and control design of a horizontal shaft magnetic bearing system," *IEEE Trans. Magnetics*, vol MAG-22, no. 3, May 1986, pp. 196-203.

[12] J. H. S. Osman and P. D. Roberts, "Two Level Control Strategy for Robot Manipulators," *Int. Journal of Control*, vol. 61, no. 6, June 1995, pp. 1201 – 1222.